

Diamond-sensing microdevices for environmental control and analytical applications

W.Haenni^a, H.Baumann^b, Ch.Comninellis^c, D.Gandini^c, P.Niedermann^a,
A.Perret^a, N.Skinner^a

^a CSEM, Centre Suisse d'Electronique et de Microtechnique SA, Rue Jaquet-Droz 1, CH 20071 Neuchâtel, Switzerland

^b Institut de Physique, Université de Neuchâtel, CH 2001 Neuchâtel, Switzerland

^c Institut de Génie Chimique, EPFL, Ecublens, CH-1015 Lausanne, Switzerland

Received 23 July 1997 ; accepted 16 September 1997

Abstract

For the fabrication of microdevices with line widths approaching 1 μm , a patterning methodology has been developed by the modification of an existing plasma etching process, which is suitable for any form and type of diamond.

These microdevices have been tested as active sensing elements for both environmental control and metrological applications: voltammetric detection of chlorine, detection of atomic oxygen for space and terrestrial applications, the measurement of ultraviolet (UV) light, and finally, conductive atomic force microscopy (AFM) which is successfully performed today with microfabricated diamond tips.

Keyword: Applications, Diamond films

1. Introduction

For several years, CSEM has been active in the development of thin, structured and conformal carbon based films like amorphous carbon (resistivity, ρ , a-C, $<3 \times 10^{-3} \Omega\text{cm}$), diamond like carbon (DLC, $\rho > 10^{10} \Omega\text{cm}$) and polycrystalline, boron doped diamond ($\rho > 0.1 \Omega\text{cm}$) for membranes, gas and thermal sensors, precision mechanics, either as discrete devices or as parts of microsystems [1,2].

Nevertheless, the fabrication of devices with functional carbon based films, especially diamond, requires simple adaptable and high resolution structuring techniques compatible with standard silicon technology. Up to now, diamond coatings could only be structured with selective area deposition techniques [1-5]. Line-widths down to 2.5 μm with a pitch of 5 μm were obtained. It has been shown by different authors that the realisation of an even smaller line-width or pitch will be extremely difficult. The structuration of blanket diamond coatings by reactive ion etching (RIE) has been reported by several authors [1,6,7]. Unfortunately, heavily doped diamond (ρ 0,1 to $1 \Omega\text{cm}$) films could not be successfully structured with this method up to now.

The electrical conductivity and different sensor behaviour of boron doped diamond has been demonstrated. [8,9] have previously presented the use of conductive diamond coatings for tips in nanoprobe experiments. While the topography

image of graphite samples in a contact-mode AFM measurement does not show structure, the conductivity image with a diamond coated silicon-tip reveals the atomic periodicity of graphite.

The functionality of boron doped diamond as an electrode material in electrochemical applications has been reported by [10,11]. It displays a wide water decomposition window relative to platinum and glassy carbon. Furthermore, due to the diamond's negative temperature coefficient (NTC) and piezo-resistive characteristic it can be exploited in environmental control: thermistors in flow transducers [12] or as pressure gauges.

Another property of interest is diamond's optoelectrical conductivity [13]. Undoped diamond film UV sensors show a quantum efficiency near 1 if exposed to UV light at less than 230nm where a sharp drop in electrical resistance induced over several decades is included.

The Schottky diode and the MISFET behaviour have also been demonstrated [14-16]. Finally, author [17] is using a combination of Pd/i-diamond/p-diamond as a hydrogen gas sensor in which the presence of hydrogen modifies the I-V and C-V characteristics of the device.

2. Experimental

2.1 Diamond film

Diamond films are conformally grown on flat or structured silicon or silicon/silicon nitride substrates and in some cases on silicon dioxide or molybdenum, by the hot filament technique

(HFCVD) at a deposition rate of 0.3 $\mu\text{m}/\text{h}$ and in the temperature range 760 to 870 $^{\circ}\text{C}$. The boron dopant is introduced in the diamond film by in-situ doping during the CVD process through a trimethyl-boron (TMB) gas source. This HFCVD process produces a columnar, random textured, polycrystalline film with a surface dominated by {111} facets giving a roughness $R_a = 50\text{--}70\text{ nm}$ for 1 μm thick layers. The electrical conductivity is $<0.2\ \Omega\text{cm}$ for highly doped diamond films representing boron doping concentration of $3\cdot 500\text{ ppm}$ or $10^{20}\text{ atoms}/\text{cm}^3$.



Fig. 1. SEM picture of a fracture of a RIE structured boron doped diamond film

2.2 Structuration

The structuration of intrinsic diamond films for device fabrication can be done either by selected area deposition or by RIE [1]. However, in practice the selected area deposition technique has shown a resolution limitation of 2.5 μm line width and a pitch of 5 μm whereas the RIE- technique with oxygen showed line- and space widths of 2 μm . Selectively deposited diamond films can be obtained independent of the doping material and concentration. Unfortunately, boron-doped diamond films could not be etched up to now with a high selectivity with respect to the mask and to the desired patterning level under standard plasma conditions. For the fabrication of diamond microelectrode arrays, line- and space-widths down to 1 μm and with high yield and reproducibility are necessary.

A modified plasma etching process which is suitable for any form and type of diamond has been developed. Diamond films were first uniformly overcoated with a thin (about 200 nm thick), densified silicon dioxide film. Standard photolithography is performed to pattern the silicon dioxide coating through a dry or wet etch. The final plasma process for the structuration of the diamond film involves RIE with an oxygen plasma. In figure 1, the underetching of the diamond film is better than 0.2 μm . The selectivity of the etching process of diamond versus silicon, silicon nitride and silicon

dioxide is better than 50 to 1 and the diamond etch rate is 150 nm/min (250 W), (Figure 2).

2.3 Device finishing

The structured diamond films are processed afterwards, if necessary by applying insulating or passivating overlayers such as silicon dioxide, silicon nitride or DLC. Patterning is performed via a plasma process or a wet etch. For ohmic contacts on boron doped diamond, a TiW/Al (150/800 nm) film is sputtered and annealed at 420 $^{\circ}\text{C}$. Even more sophisticated structures can be implemented, as for example the gas sensor shown in figure 3.

3. Results and Discussion

3.1 AFM diamond tips

Conical or pyramidal silicon tips with a continuous and conformal HFCVD boron doped diamond coating of 100 nm thickness (the lowest to ensure good homogeneity) have been demonstrated earlier [8]. The scanning electron microscope (SEM) image in figure 4 shows a coated commercially available AFM tip (Nanosensors, D-35578 Wetzlar-Blankenfeld) and demonstrates that the coverage is continuous, even for a very thin diamond film. It also displays the typical granular structure of the polycrystalline film leading to a roughness on the sub-100 nm scale with sharp edges, so that on a flat surface, high resolution AFM imaging can still be obtained. Pure diamond tips of pyramidal shape have also been demonstrated, fabricated by deposition in a micromachined mould [8]. They are formed using a mould with a 1 μm HFCVD diamond film in Si (111) pyramidal pits routinely resulting in tips with 10 to 40 nm apex radius.

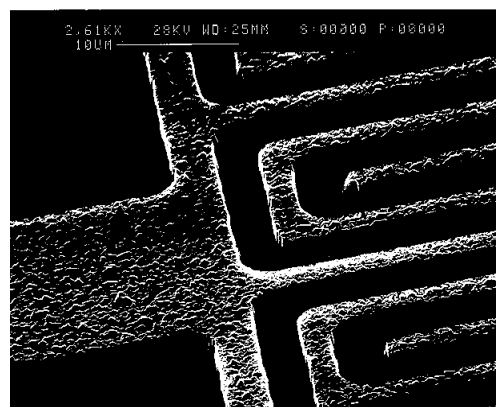


Fig. 2. SEM picture of a RIE structured boron doped diamond film

Recently, such pyramidal tips have been integrated with HFCVD diamond cantilevers, as shown in figure 5. The diamond pyramids are also formed by moulding in Si (111) trenches. The

diamond was either selectively deposited in order to simultaneously form the tips and cantilevers with the aid of a silicon dioxide mask, or structured by RIE as described in section 2. Finally, the silicon was removed by etching in KOH. Again, tip wall and cantilever thickness were 1 μm . The V-shaped cantilevers with lengths ranging from 100 to 500 μm had spring constants from 0.1 to 10 N/m. The softest cantilevers had a resonance frequency of 11 ± 3 kHz, as predicted using literature values of the Young's modulus for polycrystalline diamond, being 1050 GPa. Test structures showed the free-standing diamond films to be under a compressive

strain of 1×10^{-4} . A preliminary test, demonstrating the excellent electrical contact properties of these devices, has been performed. A conducting AFM experiment is shown in figure 6, taken on a step on a silicon substrate with a selectively grown boron doped diamond layer, as was used to fabricate the devices themselves. This experiment was performed in air at relatively low forces ($\sim 10^{-7}$ N). The bright areas have a contact resistance of less than 1 M Ω . Lower contact resistances could probably be obtained by increasing the contact force. The passivated silicon substrate does not produce a leakage current.

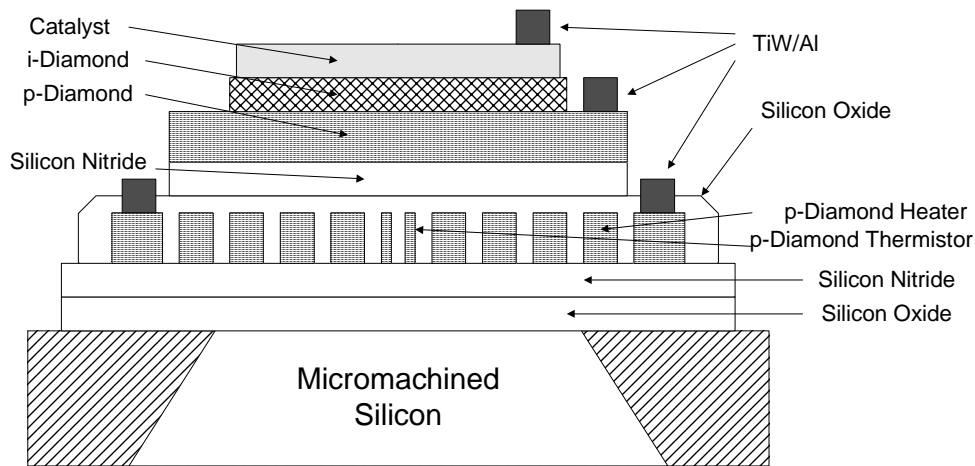


Fig. 3. Schematic view of a gas sensor device with an integrated diamond heater

3.2 Micro electrodes

Very promising results of the enlarged voltage domains of carbon-based electrodes relative to platinum and glassy carbon have been reported [10]. Amorphous carbon (a-C) and boron doped diamond electrodes have been tested under various conditions. Figure 7 shows a voltammogram obtained with such electrodes. a-C and diamond have a large overpotential showing similar behaviour on the cathodic side, allowing the reduction of heavy metals before hydrogen appears.

On the anodic side, diamond electrodes allow the direct oxidation of organic compounds like phenol to carbon dioxide and water without forming intermediates like quinones. Furthermore, the cathodic side allows also the polarographic determination of chlorine without oxygen formation. A further advantage of diamond is that its surface is less prone to surface fouling. This presents a major potential advantage relative to existing technologies where membranes are a prerequisite in order to control mass transfer of analyte to the electrode surface.

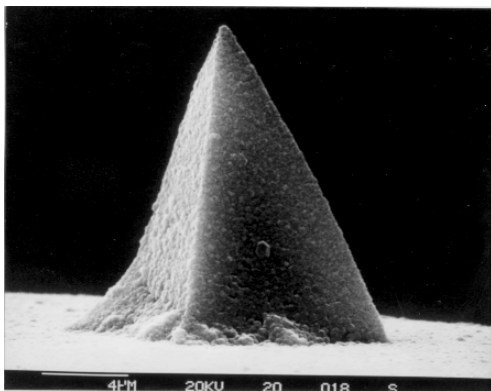


Fig. 4. Commercially available Si-tip with a boron doped diamond coating

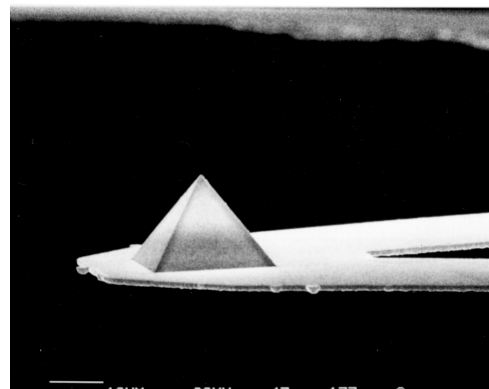


Fig. 5. Self-standing Diamond cantilever with integrated pyramid

Interdigitated voltammetric diamond microelectrode arrays lend themselves to new applications in the analytical and electrochemical fields where standard electrodes (such as platinum) can only be used with membranes. For this application, very narrow line-

widths down to 1 μm are necessary. Figure 8 shows such a microelectrode array. The redox-cycling characterisation of these microelectrode arrays is currently underway..

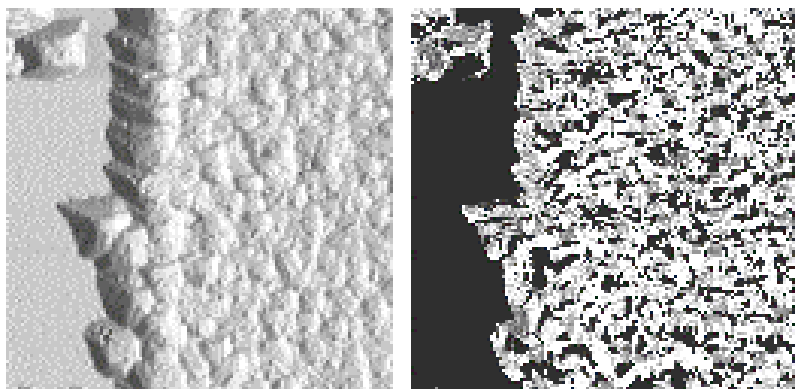


Fig. 6. AFM images of a selective area deposited 1- μm diamond coating on silicon. Left, topography; right, conductivity on a 10 x 10 μm area

3.3 Atomic oxygen sensor (for high vacuum and space applications)

Diamond is a combustible material like graphite and a-C. Graphite and a-C are currently used as atomic oxygen sensor materials for space applications but have relatively high etching rates (some hours to some days). It is supposed that diamond will also be consumed by bombardment with atomic oxygen under space conditions but with a lower etching rate, and, due to this fact, will be used as a sensor material for longer flight missions. For this purpose, boron doped diamond Wheatstone bridge elements, such as those described in a recent paper [1], have been tested as an atomic oxygen

sensor material in the ESTEC ATOX facility. The results are presented in Figure 9. Three separate devices with 10, 50 and 96 squares, representing about 0.75, 4.8 and 10 $\text{k}\Omega$ resistors respectively, have been simultaneously exposed to simulated atomic oxygen (AO). During exposure, measurements have been taken of the electrical resistance across the four junctions of each of the Wheatstone bridge devices to study the behaviour of the device in the presence of AO. Each device has four resistive sites between the junctions. Two of these sites are exposed to AO whereas the two others, opposite to the first ones, are protected by a silicon dioxide/nitride double-layer.

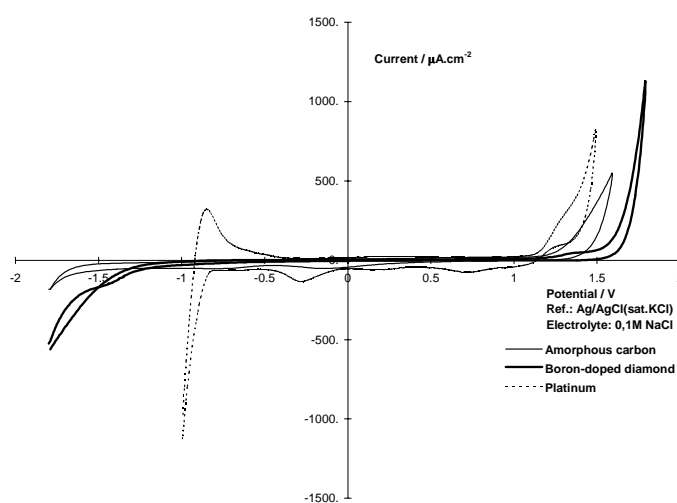


Fig. 7. Voltammogram of platinum, a-carbon and boron doped diamond

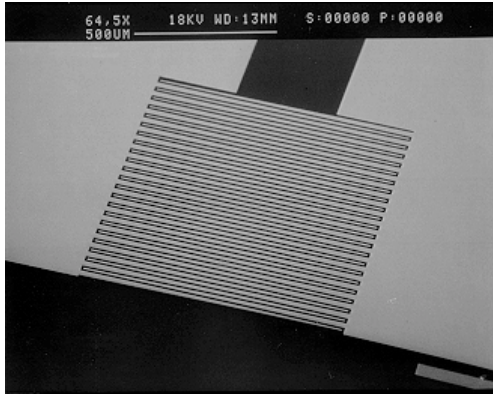


Fig. 8. Boron-doped diamond microelectrode array.

This arrangement allows the effects of temperature to be isolated from the effects of AO on the device resistance. Analysis of the effects of AO on device resistance is complicated by the fact that each of the six resistance measurements (one for each arm, a,b,c,d, and two additional ones between the two branches, a+b, c+d, of the bridge) are a combination of parallel resistors from the directly exposed and masked resistive sites. To extract the data of most interest from the six resulting simultaneous equations requires algebraic manipulation leading to the characteristic ratio: $[b+d]/[a+c]$. This ratio takes into consideration the relative AO and temperature related resistance change of the resistive sites b and d relative to the temperature related resistance changes of the sites a and c. The ratio therefore, always has a value greater than unity and only varies as a function of the AO effects on the device resistance. Results of this analysis technique show that, within the limits of experimental uncertainty (concerning the incremental measurement of cumulative AO flux), the resistance of the exposed resistive sites in each device increases linearly with AO exposure flux. In addition, there does not appear to be any recovery of the devices initial resistance after exposure which suggests that a limiting device lifetime may be reached under continued exposure to AO.

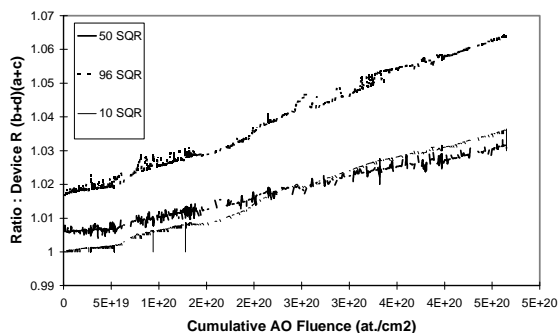


Fig. 9. Bulk resistivity behaviour of diamond due to etching in an atomic oxygen flux.

3.4 Oxygen radical sensor (ambient air applications)

The photoelectrical behaviour of doped and undoped, 1 μm thick diamond films has been evaluated. For these measurements, microdevices with interdigitated metallic electrodes ohmically contacted to diamond with different line and space widths have been prepared. The electrical resistivity of diamond changes dramatically over several decades if exposed to UV-light below 230 nm, consistent with the observation of [13]. Additional but smaller resistivity changes occur at higher wave lengths due to nitrogen or boron doping. It has been previously determined that the electrical conductivity of diamond consists of two different contributions the former from the bulk and the second from the surface. In fact, during the measurements, a superimposed electrically resistive change in the device occurred when the UV-light was switched on. The same measurements have been repeated with the Wheatstone-bridge elements used for the AO experiments. The phenomenon was also observed on the unprotected resistors but not on the protected (reference resistor) ones. Ref. [14] indicates, that diamond's surface conductivity changes if exposed to ozone. Strong UV-light sources also produce ozone.

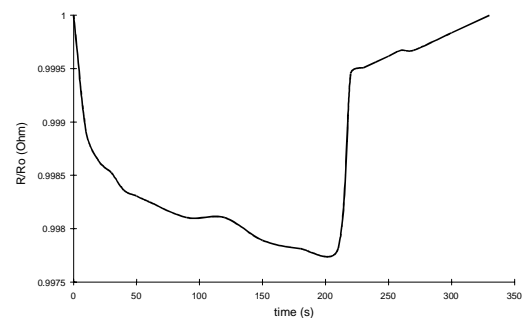


Fig. 10. Surface resistivity sensing behaviour of diamond in the presence of oxygen radicals, generated from nitric acid.

Additional investigations are still needed in order to study the behaviour of diamond's surface conductivity in the presence of oxygen radicals, such as those produced by ozone, nitric acid (NO/NO_2) and combustion gases (NO_x). Figure 10 demonstrates the perfect reversibility of the surface conductivity behaviour of diamond toward oxygen radicals generated by nitric acid. The ambient relative humidity (RH) from 20 to 95 % does not influence the surface conductivity of diamond in any way. To understand this selectivity further analytical work will be performed.

4. Conclusion

An alternative to using selective area deposition to structure diamond coatings, is a process based on

a modified oxygen plasma etching (RIE). This newly developed method allows the structuration of diamond down to line- and space-widths of 1 μm against about 3 μm with the conventional selected area deposition process. This process demonstrates superior reliability and can be used for any form and type of diamond film.

AFM silicon tips can now be conformally coated with a 100 nm thick boron doped diamond layer. Such microdevices are now commercially available. Mould coated, pyramidal diamond tips, having an apex radius of 10 to 40 nm which is 5 to 10 times smaller than the coated silicon tips, have been demonstrated. Such pyramidal mould coated diamond tips can be integrated in self standing diamond cantilevers with spring constants from 0.1 to 10 N/m and a resonance frequency up to 10 kHz. They will be used for metrological applications with no detectable degradation.

Due to the large overpotential relative to platinum, diamond electrodes provide a means of directly oxidising organic compounds to carbon dioxide without forming intermediates. Its surface does not show any degradation during this process. The polarographic determination of chlorine is possible without oxygen formation.

It has been revealed that diamond is a potential atomic oxygen sensing device for space as well as for terrestrial applications. The electrical resistivity of boron doped diamond resistors increases linearly with atomic oxygen flux under vacuum conditions without a surface transformation which could limit the response or the lifetime of the device. Under ambient air conditions, oxygen radicals from ozone or nitric acid reversibly change the electrical surface conductivity of diamond. This sensing behaviour may be used for device fabrication.

Acknowledgement

The authors are grateful to Marc Van Eesbeek and Jeremy Matcham from ESA/ESTEC, NL-Noordwijk, for the atomic oxygen measurements and characterization of the sensor.

References

- [1] W.Haenni, J.P.Dan, A.Perret, J.P.Thiébaud, P.Weiss, Application of Diamond Films and Related Materials: Proceedings, Third International Conference, NIST SP 885 (1995) 83
- [2] A.Perret, W.Haenni, X.M.Tang, P.Niedermann, MST-News, (1997), to be published
- [3] I.Taher, M.Asalam, M.A.Tamor, T.J.Potter, R.C.Elder, Sensors and Actuators A 45 (1994) 35
- [4] M.C.Kwan, K.K.Gleason, Diamond and Relat. Mater., 5 (1996) 1048.
- [5] P.G.Roberts, D.K.Milne, P.John, M.G.Jubber, J.I.B.Wilson, J.Mater.Res., 11 (1996) 3128
- [6] B.Miller, R.Kalish, L.C.Feldmann, A.Katz, N.Moriya, K.Short, A.E.White, J. Electrochem. Soc., 141 (1994) 141
- [7] B.R.Stoner, G.J.Tessmer, D.L.Dreifus, Applied Physics Letters 62 (1993) 1803
- [8] P.Niedermann, W.Haenni, N.Blanc, R.Christoph, R.Burger, J.Vac.Sci. Technol., A 14 (1996) 1233
- [9] W.Kulisch, A.Malave, G.Lippold, W.Scholz, C.Milalcea, E.Oesterschulze, Diamond and Relat. Mater., 6 (1997) 906
- [10] H.B.Martin, A.Argonita, U.Landau, A.B.Anderson, J.C.Angus, J. Electrochem. Soc., 143 (1996) L133
- [11] J.J.Carey, C.S.Christ, S.N.Lowery, US-Patent 5'399'247, March 21, 1995
- [12] M.Binggeli, J.P.Dan, A.Grisel, W.Haenni, H.E.Hintermann, P.Krebs, C.Mueller, Proceedings, 2nd International Conference on the Application of Diamond Films and Related Materials, MYU, Tokyo (1993) 51
- [13] R.D.Mc Keag, M.D.Withfield, S.S.Chan, L.Y.Pang, R.B.Jackmann, Mat. Res. Soc. Symp. Proc., 416 (1996) 419
- [14] W.Ebert, A.Vescan, P.Gluche, T.Borst, E.Kohn, Diamond and Relat. Mater., 6 (1997) 329
- [15] L.Y.S.Pang, S.S.M.Chan, C.Johnston, P.Chalker, R.B.Jackmann, Diamond and Relat. Mater., 6 (1997) 333
- [16] B.A.Fox, M.L.Hartsell, D.M.Malta, H.A.Wynands, G.J.Tessmer, D.L.Dreifus, Mat.Res. Symp. Proc., 416 (1996) 319
- [17] Y.Gurbuz, W.P.Kang, J.L.Davidson, D.L.Kinser, D.V.Kerns, Sensors and Actuators, B33 (1996) 100